

Quantitative analysis of density-dependent transport in tetramethyltetraselenafulvalene single-crystal transistors: Intrinsic properties and trapping

H. Xie,^{1,2} H. Alves,³ and A. F. Morpurgo^{2,*}¹*Kavli Institute of NanoScience, Delft University of Technology, 2628CJ Delft, The Netherlands*²*DPMC and GAP, University of Geneva, 24 quai Ernest-Ansermet, CH1211 Geneva, Switzerland*³*INESC-MN and IN, Rua Alves Redol 9, 1000-029 Lisboa, Portugal*

(Received 30 September 2009; published 4 December 2009)

We perform a combined experimental and theoretical study of tetramethyltetraselenafulvalene (TMTSF) single-crystal field-effect transistors, whose electrical characteristics exhibit clear signatures of the intrinsic transport properties of the material. We present a simple, well-defined model based on physical parameters and we successfully reproduce quantitatively the device properties as a function of temperature and carrier density. The analysis allows its internal consistency to be checked, and enables the reliable extraction of the density and characteristic energy of shallow and deep traps in the material. Our findings provide indications as to the origin of shallow traps in TMTSF transistors.

DOI: [10.1103/PhysRevB.80.245305](https://doi.org/10.1103/PhysRevB.80.245305)

PACS number(s): 72.80.Le, 73.40.-c, 73.90.+f

I. INTRODUCTION

Despite impressive progress in the use of organic semiconductors for the realization of practical circuits and devices, our fundamental understanding of these materials remains limited. In this context, the recent observation in organic single-crystal field-effect transistors (FETs) (Ref. 1) of an anisotropic carrier mobility increasing with lowering temperature^{2,3} represents a breakthrough: it demonstrates that the intrinsic transport properties of organic semiconductors can be accessed experimentally in a transistor configuration, at finite and tunable density of charge carriers. The investigation of these properties is the motivation for much effort that is being devoted to increase the purity of molecular semiconductors,⁴ to broaden the scope of organic crystals enabling the realization of high-quality organic FETs,⁵⁻⁷ to improve the level of material characterization,⁸ and to perform investigations of specific transport phenomena.⁹⁻¹⁴ Indeed, thanks to the quality of organic single-crystal transistors,¹⁵⁻¹⁷ experimental results can now be reproduced in different laboratories in quite some detail (which is less commonly the case for thin-film FETs used in applications), making it possible to compare measurements on the same experimental system performed by different groups and based on different techniques. This is a key step to reach a true microscopic understanding of molecular semiconductors.

In order to establish a firm basis for such a microscopic understanding, it is important that experimental investigations are carried out in conjunction with a *quantitative* interpretation of the data. Only in this way, detailed cross-checks between different experiments and their interpretation can be performed, as it is needed to verify the physical assumptions on which our microscopic understanding is founded, and their internal consistency. A quantitative analysis and cross-checks are now possible, and considerable part of our activity over the past few years has been motivated by this goal.

Two cases in which this quantitative analysis has been successful are the following. One example is provided by the study of transport of charge carriers accumulated in the chan-

nel of rubrene FETs with different gate dielectrics.⁹ A quantitative and systematic analysis of these experiments has shown that, when the dielectric is highly polarizable, charge carriers at the organic/dielectric interface form Fröhlich polarons.¹⁰ The validity of this conclusion has been cross-checked by extending the experiments and the theoretical analysis to the high carrier density regime, where the effect of Coulomb interactions between carriers becomes important. In this regime, new phenomena—a saturation of the source-drain current and an increase in the activation energy of the mobility with increasing density of charge carriers—were observed, and could be interpreted quantitatively in terms of interacting Fröhlich polarons, without the introduction of new parameters in the theory.¹⁸

The second example is provided by work from different groups that has analyzed quantitatively optical conductivity data,¹² transport at metal/organic interfaces,¹⁹ and the band profile in Schottky transistors.²⁰ From this work, several microscopic parameters have been rather accurately extracted, such as the effective mass of charge carriers in rubrene, the remnant density of dopants in high-purity rubrene crystals, and the height of the Schottky barrier at (oxidized) Copper/rubrene interfaces. Subsequently, using these results, it has been possible to model charge transfer at oxidized-Copper/rubrene interfaces quantitatively, without introducing any free parameter, finding a remarkably good agreement between theory and experiments.²¹

Despite these successes, a systematic quantitative analysis of experiments in devices exhibiting bandlike transport, with the mobility $\mu(T)$ increasing with lowering temperature, has not been performed yet. In large part, this is due to the lack of a well-defined theoretical framework enabling a quantitative study in this regime. In fact, past work on the bandlike transport regime of (bulk) organic semiconductors—based on time-of-flight measurements²²—has relied on the so-called trap-and-release model^{22,23} that, although helpful,²⁴ cannot be applied to the systematic analysis of systems at finite carrier density. In field-effect transistor experiments, this lack of a suitable framework to analyze quantitatively the bandlike regime is preventing a detailed understanding.

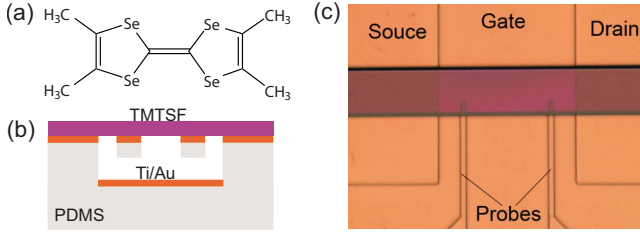


FIG. 1. (Color online) (a) Chemical structure of TMTSF molecule. (b) Schematic cross section of our PDMS-based TMTSF transistors. (c) Optical microscope image of a TMTSF PDMS FET (the separation between source and drain is $300 \mu\text{m}$).

For instance, it prevents a precise description of the interplay between delocalization of charge carriers and trapping still present even in the best devices.

It is also important to extend the exploration of the intrinsic properties of organic semiconductors to materials other than rubrene, which is the only one so far in which a metalliclike temperature dependence of the mobility in a FET configuration has been observed. Indeed, to understand which properties of molecular semiconductors are common to all materials, and which are characteristic to a specific molecule, a comparison of data obtained from crystals of many different molecules is certainly required. Furthermore, the identification of new molecular materials with increasingly higher quality is needed to push to lower temperature range in which the intrinsic transport properties dominate. This is crucial to enable the study of organic semiconductors with a higher energy resolution.

To start addressing these issues, here we report a combined experimental and theoretical study of transport through tetramethyltetraselenafulvalene [TMTSF, $\text{C}_{10}\text{H}_{12}\text{Se}_4$, see Fig. 1(a)] single-crystal FETs. We first show that these devices exhibit the characteristic signatures of the intrinsic transport properties. We then present a simple model based on physically transparent quantities and assumptions, with which we analyze in detail the temperature and density dependence of the mobility, as well as the temperature dependence of the threshold voltage. Our analysis reproduces the observations systematically and quantitatively, it gives consistent results on different devices, and it allows us to check its internal consistency. From the analysis, we extract the concentration and characteristic energy of traps, and we are able to draw detailed conclusions on how traps at different energy affects the device response. Finally, we also obtain indications as to the physical origin of shallow traps in TMTSF FETs. At a more general level, the results presented clearly indicate that the model represents an appropriate framework for the analysis of transport through high-quality organic FETs.

II. EXPERIMENTAL RESULTS

So far, rubrene crystals have been the only ones to unambiguously show the expected signatures of intrinsic transport at finite carrier density in a FET configuration.¹ We have explored crystals of different molecules, and here we discuss TMTSF transistors,^{25,26} realized by laminating single-

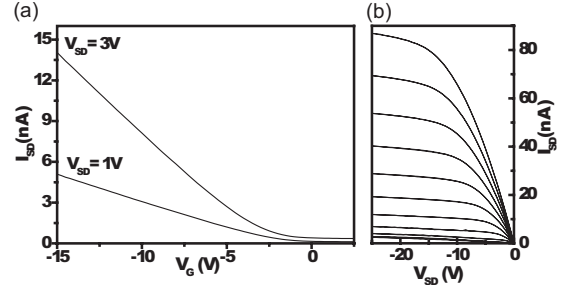


FIG. 2. Panel (a) shows the source-drain current, measured at room temperature, as a function of gate voltage, for two values of source-drain voltage ($V_{SD}=1$ and 3 V). Panel (b) shows the source-drain current as a function of source-bias voltage, for different values of V_G (from -1 to -19 V , in -2 V steps). These measurements were taken on device S1 whose mobility and threshold voltage data are shown in Fig. 4.

crystals grown from vapor phase transport onto a polydimethylsiloxane (PDMS) support. The schematics of the transistors are shown in Figs. 1(b) and 1(c): gold is the contact material, and the device configuration is such that the crystal is suspended on top of the gate, with vacuum acting as a gate dielectric (the fabrication procedure of these devices is identical to that described in Ref. 27). Figure 1(c) shows an optical micrograph of one of our devices. Immediately after fabrication, the transistors were transferred into the vacuum chamber ($p \approx 2 \times 10^{-7} \text{ mbar}$) of a flow cryostat where all transport measurements were done. Most measurements were taken using a HP 4156A parameter analyzer, in a four-terminal configuration [Fig. 1(c)], to eliminate the effects of the contact resistance. We discuss data taken on three different FETs, representative of the approximately 10 devices studied.

Figure 2 shows the electrical characteristics of one device, measured at room temperature, in a two-terminal configuration. Both the source-drain current I_{SD} measured as a function of V_G [for fixed V_{SD} , Fig. 2(a)], and the measurements of I_{SD} as a function of source-drain voltage V_{SD} [for different values of V_G , Fig. 2(b)], exhibit ideal characteristics (no hysteresis, absence of nonidelaities due to contact effects, well-defined saturation regime). The devices are stable and reproducible. These observations provide a first indication of the high-quality of TMTSF single-crystal FETs.

Systematic measurements at different temperatures were performed in a four-terminal configuration, to ensure that the contact resistance (which is expected to increase as the temperature is lowered) does not affect the results. The transfer characteristics obtained in this way are shown in Fig. 3, from which we extract the full temperature dependence of the mobility. The value of μ is extracted from the linear part of the I_{SD} - V_G characteristics, using the relation $\mu = (L/W)(1/C_i)(1/V)(dI_{SD}/dV_G)$ (with L separation between voltage probes, W crystal width, C_i gate capacitance per unit area, and V voltage difference measured between the two voltage probes). At room temperature, $\mu=4 \text{ cm}^2/\text{V s}$ reproducibly in many different devices (approximately 10; the same value is obtained from the I_{SD} - V_{SD} characteristics in the saturation regime, measured in a two-terminal configuration), comparable to what has been reported in Ref. 26. From

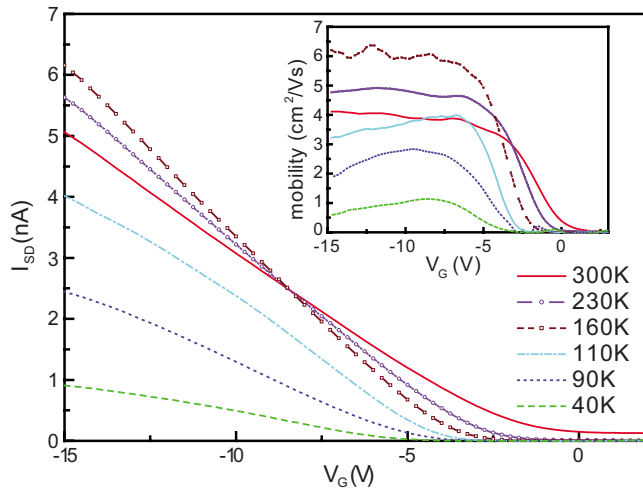


FIG. 3. (Color online) Transfer characteristics (I_{SD} - V_G) measured on a high-quality TMTSF single-crystal FET, at different values of temperature. The inset shows the gate-voltage dependent mobility extracted from these measurements. These measurements were taken on device S1 whose mobility and threshold voltage data are shown in Fig. 4.

the I_{SD} - V_G curves, we also extract the temperature dependence of the threshold voltage $V_T(T)$, by extrapolating the curves to zero current.

Figures 4(a) and 4(b) show the mobility and threshold voltage as a function of temperature measured on three dif-

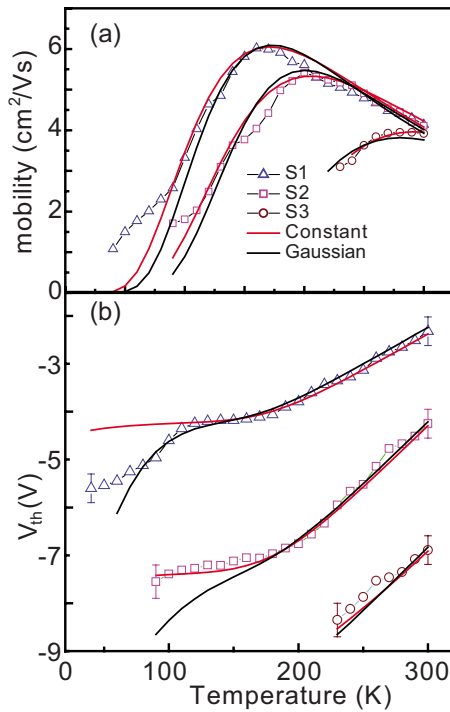


FIG. 4. (Color online) In panels (a) and (b), the symbols represent the temperature dependent mobility (a) and threshold voltage (b) measured on three different devices. The solid lines represent the result of our model, using the parameters listed in Table I; the red and black lines are obtained using a constant and a Gaussian density of shallow traps, respectively.

ferent samples that we have investigated in most detail. The mobility tends to increase, exhibiting an identical temperature dependence down to a sample-dependent temperature value, after which μ decreases with further lowering T . In the temperature interval where $\mu(T)$ is “metalliclike,” the $\mu(T)$ curves measured in different samples overlap, indicating that we are indeed probing the intrinsic material properties. The different extents of this interval in different samples indicate that the amount of disorder present is different. Interestingly, the decrease in the mobility at low T is very slow. In our best sample, μ reaches a value above $6 \text{ cm}^2/\text{V s}$ at $T \approx 160 \text{ K}$, and it is still close to $2 \text{ cm}^2/\text{V s}$ at 50 K , which is unusually large for organic transistors at these low temperature values.

The behavior of the threshold voltage is qualitatively similar in different devices. It exhibits a linear decrease with lowering T at first, and a tendency to saturate at lower T . The magnitude of V_T depends on the sample, again indicating that different amounts of disorder are present in the different samples. Interestingly, the behavior of the threshold voltage in different devices correlates with the behavior of the mobility, with the magnitude of V_T being systematically larger in devices that exhibit the intrinsic transport properties down to a lower temperature. Although such a correlation may not appear “strange” at a first glance—since both lower mobility and larger threshold voltage are indicative of higher disorder—it does contain valuable microscopic information (see the Discussion Section). To emphasize the relevance of this point, we note that comparison of the characteristics of rubrene single-crystal FETs before and after the crystals were irradiated with x-rays have shown that x-ray irradiation leads to a substantial increase in threshold voltage, but no change in mobility.³ In other words, a correlation between threshold voltage and temperature dependence of the mobility observed in TMTSF single-crystal FET was not reported in rubrene devices.

III. DETAILS OF THE THEORETICAL ANALYSIS

We now proceed to discuss the strategy that we follow to analyze quantitatively the data. To this end, we present a simple model based on the assumption that transport of holes in TMTSF occurs in a band, with density of states N_0 for energy $E > 0$. Disorder-induced trap states are also present for $E < 0$, and consist of shallow traps with density of states $N_S(E)$, and deep traps located much deeper in energy, described by a density of states $N_D(E)$ (see also Ref. 28). The mobility of carriers occupying states in the band is the intrinsic mobility in the material, and, following existing theories, is assumed to depend on temperature as $\mu_0(T) = \alpha T^{-2}$.²⁹⁻³¹ Carriers occupying trap states are assumed not to carry current.

In practice, we fix the shape of the density of states and calculate the position of the Fermi level E_F (numerically) as a function of the total density of accumulated charge $n (=C_i V_G)$ through the relation

$$n = \int_0^{+\infty} N_0 \frac{1}{e^{E-E_F/kT} + 1} dE + \int_{-\infty}^0 [N_S(E) + N_D(E)] \frac{1}{e^{E-E_F/kT} + 1} dE \quad (1)$$

that defines E_F . Having determined $E_F(n, T)$, it is straightforward to obtain the source-drain current I_{SD} in terms of the density of charge carriers occupying states in the band ($n_C(n, T) = \int_0^{+\infty} N_0 \frac{1}{e^{E-E_F/kT} + 1} dE$) as

$$I_{SD}(n = C_i V_G) = n_C(n, T) e \mu_0(T) \frac{W}{L} V_{SD}. \quad (2)$$

From Eq. (2), we extract all quantities that are measured in the experiments by applying to the calculated I_{SD} - V_{SD} curves the same procedures used for the measured ones. For instance, the mobility μ measured from the FET characteristics is simply given by $\mu = \mu_0(T) \frac{\partial n_C(n, T)}{\partial n}$ (which corresponds to $\mu \propto \frac{\partial I_{SD}}{\partial V_G}$).

For our calculations, we use, for the shallow traps, a constant density of states [$N_S(E) = N_c = \text{const}$, if $E_c < E < 0$, and $N_S(E) = 0$ otherwise], and a Gaussian density of states ($N_S(E) = N_g e^{-(E/2E_g)^2}$), and compare the results obtained, under the condition that the total number of shallow traps $\int_{-\infty}^0 N_S(E) dE$ is the same for the two distributions. For the deep traps, we use a “square” distribution [$N_D(E) = N_D = \text{constant}$ if $E_D - \delta E_D/2 < E < E_D + \delta E_D/2$ and zero otherwise] to analyze the role of the trap depth (E_D) and of the distribution width (ΔE_D). The density of states in the band at the surface of the TMTSF crystal— $N_0 = 10^{15} \text{ cm}^{-2} \text{ eV}^{-1}$ —is estimated by taking one state per molecule distributed in energy over the bandwidth of the valence band ($\approx 0.5 \text{ eV}$).³² The parameter α [in the expression $\mu_0(T) = \alpha T^{-2}$] represents an intrinsic property of TMTSF crystals, and it is therefore taken to be the same for all samples.

A strategy similar to the one adopted here—i.e., “fixing” a density of states to analyze transport through FETs—is used to describe transport in FETs based on amorphous materials.^{28,33} In that case, however, transport is due to carriers occupying localized states, whose mobility is strongly energy dependent, and material inhomogeneity requires percolation effects to be taken into account.³⁴ This significantly increases the complexity of the analysis, as well as the unambiguous extraction of parameters in the model. In fact, the functions describing the energy-dependent density of states and mobility are not known, and considerable freedom is left in selecting one specific functional dependence. In addition, the reproducibility of transistors based on amorphous materials used in earlier investigations was not as good as in high-quality single-crystal transistors. As we will show, all these problems are absent in high-quality single-crystal FETs, whose characteristics can be analyzed precisely in a broad temperature range, enabling—among other things—the internal consistency of the theoretical analysis to be verified.³⁵

IV. DISCUSSION

Our analysis is limited to a temperature range where a significant fraction of carriers populate states in the band, corresponding, for the best devices, to temperatures higher than approximately 100 K. In this regime, the model shows that the behavior of the temperature dependence of the mobility $\mu(T)$ measured at high carrier density depends only on the properties of the shallow traps [Fig. 4(a)], whereas the behavior of $V_T(T)$ is determined only by the deep traps [Fig. 4(b)]. This conclusion, which is a consequence of the fact that in high-quality organic FETs shallow and deep traps are well-separated in energy, considerably simplifies the analysis of the data. As we will discuss, the model reproduces quantitatively all measured properties of the devices satisfactorily, and, only at temperatures such that most carriers occupy trap states ($T < 100 \text{ K}$ for the best devices), the model starts to deviate from the experiments. The deviations are due to the fact that, contrary to our assumption, carriers in shallow traps can still give a contribution to the current. As we will argue in the end, this is consistent with the physical picture for the origin of the shallow trap states that emerges from our analysis (see also Ref. 38).

We start by discussing the temperature dependence of the mobility. As explained above, we consider different energy distributions for the shallow traps (constant and Gaussian),³⁶ since these allow us to establish which are the aspects of our conclusions that are physically significant. Best fits to the data with the two distributions are shown in Fig. 4(a). We see that, for the temperature range discussed above, the agreement is satisfactory.³⁶ Table I summarizes the parameters extracted from the fits. Note that the energies E_c and E_g satisfy the relation $E_c = 3E_g$ to a 10% precision (or better) for all samples, which can be easily understood since the integral of the Gaussian trap distribution between $E = 3E_g$ and $E = 0$ gives 99% of the shallow trap states. Since different distributions lead to a nearly identical temperature dependence of the mobility, we conclude that the precise energy distribution of the shallow traps cannot be extracted from the analysis. However, the fact that the total density of shallow traps and their characteristic energy ($\approx E_g$) are the same for the constant and the Gaussian distribution, implies that these quantities have true physical meaning, and that the values extracted are not influenced by details of the analysis.

Next, we analyze the threshold voltage, whose temperature dependence is determined by the deep traps. Such a microscopic analysis is meaningful in our devices, because the single-crystals are suspended on top of the gate, and the threshold voltage is therefore not affected by extrinsic effects due to phenomena taking place in the gate insulator. We find that the curve $V_T(T)$ is sensitive to both the energy and the width of the deep trap distribution. Specifically, very deep traps (whose energy is larger than roughly 0.5 eV) contribute to the threshold voltage, but do not cause a shift in the temperature range considered. In this same range, a sizable contribution to the threshold voltage shift originates from traps with energy between 100 and 400 meV, approximately, with the largest contribution coming from traps between 150–200 meV. This fact—that deep traps at different energies affect differently V_T and its shift with temperature—makes it pos-

TABLE I. Values of quantities discussed in the text. The total number of shallow traps $\int_{-\infty}^0 N_S(E)dE$ is fixed to be the same for both the constant and the Gaussian energy distributions. The typical error on the parameters is 10% or better. The value of α is the same for the three devices and is equal to $6.15 \times 10^5 \text{ cm}^2 \text{ K}^2/\text{V s}$ when using the constant density of states for the shallow traps, and to $5.98 \times 10^5 \text{ cm}^2 \text{ K}^2/\text{V s}$ when using the Gaussian density of states (i.e., the value of α that we obtain from the fits is essentially independent of the specific energy distribution of shallow traps). The corresponding values for the intrinsic mobility at room temperature ($=\alpha/(300 \text{ K})^2$) are 6.83 and 6.64 $\text{cm}^2/\text{V s}$.

	Sample 1	Sample 2	Sample 3
N_C ($\text{cm}^{-2} \text{ eV}^{-1}$)	1.97×10^{14}	8.5×10^{13}	9.3×10^{12}
E_C (meV)	38.5	54.1	111
N_g ($\text{cm}^{-2} \text{ eV}^{-1}$)	3.04×10^{14}	1.36×10^{14}	1.42×10^{13}
E_g (meV)	14.1	19.1	40.8
$\int_{-\infty}^0 N_S(E)dE$ (cm^{-2})	7.6×10^{12}	4.6×10^{12}	1.03×10^{12}
N_D ($\text{cm}^{-2} \text{ eV}^{-1}$)	6×10^{10}	1.08×10^{11}	1.08×10^{11}
E_D (meV)	225	235	270
δE_D (meV)	95	95	130
$\Delta\Phi$ (meV)	10.3	13.7	16.1

sible to extract information on the energy distribution of deep traps from the experimental $V_T(T)$ curves. With the parameter values listed in Table I, the model leads to an excellent quantitative agreement with the data (again, below approximately 100 K, where the majority of carriers occupies shallow traps, the results depend on the details of the shallow trap distribution). Note that the center of the deep trap distributions is approximately the same in the three devices. This is expected if deep traps originate from a well-defined chemical impurity hosted in the crystal. Indeed, the values of E_D and of δE_D extracted from our analysis are in the same range of energies and widths of other deep traps recently found in different molecular materials.³⁷

We note that, already, Podzorov *et al.*³ did correctly realize the link between deep traps and shift in the threshold voltage with lowering temperature. However, no quantitative analysis of this link has been done in that work. On the basis of qualitative considerations, it was stated that the data were indicative of an energy independent density of traps N_{tr} , given by $N_{tr} = C/kTe \partial V_{Th}(T)/\partial T$. From this relation, the deep trap density of states was estimated to be $\approx 10^{12} \text{ cm}^{-2} \text{ eV}^{-1}$. However, this way of estimating the density of deep traps is in general not correct, since, as we discussed above, deep traps at different energies have a very different effect on the absolute value of the threshold voltage and on its shift with lowering temperature. The fully quantitative analysis that we have performed is needed to extract the density of states of the deep traps, which, in our TMTSF single-crystal FETs, is typically one order of magnitude less ($\approx 10^{11} \text{ cm}^{-2} \text{ eV}^{-1}$; see Table I) than what was estimated in Ref. 3 for rubrene crystals.

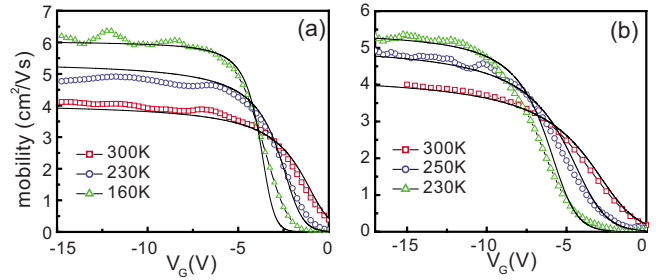


FIG. 5. (Color online) In panels (a) and (b), the symbols show the mobility extracted from FET measurements as a function of carrier density at different temperatures, on devices 1 and 3. The solid lines are calculated using the parameter values extracted from the fits shown in Fig. 4 (no other parameters need to be introduced). For device 2, a similar agreement between data and model is obtained.

With the model reproducing the experimental observations successfully, it is important to critically ask whether the quantitative agreement is not simply due to the introduction of a sufficient number of free parameters. To show that this is not the case, we have analyzed the full dependence of the mobility on carrier density at different temperature values. This comparison provides a stringent test of the validity of the model and of its consistency, because all parameters are fixed by the analysis discussed above, and no other free parameters can be introduced. Figures 5(a) and 5(b) show that the curves calculated with the model are in good quantitative agreement with the data, as long as the temperature is such that enough charge carriers are present in the band. This result confirms the internal consistency of our analysis, and illustrates that the model does describe well the interplay between bandlike transport and trapping as a function of carrier density.

Having established the internal consistency of our analysis, we address the origin of the observed correlation between the temperature dependence of mobility and of threshold voltage. Since the temperature dependence of the mobility is determined only by the shallow traps and that of the threshold voltage only by the deep traps, this correlation implies that a physical mechanism exists, that links the origin of the two kinds of traps. Several mechanisms realistically capable of establishing such a link can be envisioned. For instance, a possible scenario is that deep traps are due to impurity molecules trapped in the crystal lattice. Owing to their different size and shape, these impurities would certainly cause strain in the lattice, leading to local modification of the bandwidth in the material (since strain causes local changes in the hopping integrals between adjacent molecules). Where the bandwidth is larger, the band gap is correspondingly smaller, and local bandwidth fluctuations would cause regions of lower energy where charge carriers would tend to localize.

Here, we propose a different mechanism due to simple electrostatics. Individual charge carriers frozen in the deep traps generate random electrostatic potential fluctuations $\Delta\Phi$, and the resulting electrostatic potential landscape causes regions of lower energy in which a large density of charge carriers can be trapped. The characteristic energy scale asso-

ciated to the potential fluctuations can be estimated as $\Delta\Phi = \frac{1}{4\pi\epsilon\epsilon_0} \frac{e}{\langle r \rangle}$, where $\langle r \rangle$ is the average distance between deep traps and ϵ is the average of the relative dielectric constant of the TMTSF crystal and of vacuum. By estimating the magnitude of $\langle r \rangle$ from the total density of deep traps extracted from the fit of $V_T(T)$, we obtain the values of $\Delta\Phi$ reported in Table I, whose magnitude compares well with the characteristic energy scale E_g of the shallow traps. This scenario explains why the density of states of shallow traps at $E \approx 0$ is comparable to the density of states in the band itself. In fact, shallow traps consist of states in the band whose energy is lowered by the local, slowly varying electrostatic potential. It also explains why, below 100 K, carriers in shallow traps are seen—experimentally—to give a contribution to the conductivity, contrary to what is assumed in our model:³⁸ in fact, these carriers are not tightly bound to a defect, can move over rather large distances inside the “puddles” caused by the potential fluctuations, and contribute in this way to the local conductivity in the transistor channel. It would be certainly interesting to investigate the occurrence of correlations between threshold voltage and mobility in other materials, since this may provide information about the nature of shallow traps states, which is currently not established, and which may be different in different molecular semiconductors (for instance, as we mentioned earlier, in FETs realized with rubrene single-crystals irradiated by x-ray for different periods of time, no correlation is observed).³

V. CONCLUSIONS

In conclusion, we have developed a well-defined framework to analyze the interplay between intrinsic bandlike transport and trapping in organic single-crystal transistors at finite density of charge carriers, and we have used it to describe the behavior of high-quality TMTSF FETs. The model permits to understand in detail the physical origin of the different aspects of the device characteristics, and to extract microscopic parameters reliably. The possibility to perform internal consistency checks on the results of the analysis, as well as the precision with which parameters can be extracted, indicate that the model that we have used provide a suitable framework for the quantitative analysis of transport in organic transistors. We expect that this approach will be particularly useful in the comparative investigation of molecular semiconductors, where a quantitative analysis is important to identify unambiguously microscopic electronic properties that are common to all materials, and those that are characteristic of specific molecules.

ACKNOWLEDGMENTS

We are grateful to S. Fratini for discussions and comments, and we acknowledge financial support from NanoNed, the Swiss NCCR MaNEP, NEDO, and FCT.

*alberto.morpurgo@unige.ch

- ¹R. W. I. de Boer, M. E. Gershenson, A. F. Morpurgo, and V. Podzorov, *Phys. Status Solidi A* **201**, 1302 (2004); M. E. Gershenson, V. Podzorov, and A. F. Morpurgo, *Rev. Mod. Phys.* **78**, 973 (2006).
- ²V. C. Sundar, J. Zaumseil, V. Podzorov, E. Menard, R. L. Willett, T. Someya, M. E. Gershenson, and J. A. Rogers, *Science* **303**, 1644 (2004).
- ³V. Podzorov, E. Menard, A. Borissov, V. Kiryukhin, J. A. Rogers, and M. E. Gershenson, *Phys. Rev. Lett.* **93**, 086602 (2004).
- ⁴O. D. Jurchescu, J. Baas, and T. T. M. Palstra, *Appl. Phys. Lett.* **84**, 3061 (2004).
- ⁵A. L. Briseno, S. C. B. Mannsfeld, S. A. Jenekhe, Z. Bao, and Y. Xia, *Mater. Today* **11**, 38 (2008).
- ⁶A. S. Molinari, H. Alves, Z. Chen, A. Facchetti, and A. F. Morpurgo, *J. Am. Chem. Soc.* **131**, 2462 (2009).
- ⁷S. Haas, Y. Takahashi, K. Takimiya, and T. Hasegawa, *Appl. Phys. Lett.* **95**, 022111 (2009).
- ⁸D. V. Lang, X. Chi, T. Siegrist, A. M. Sergent, and A. P. Ramirez, *Phys. Rev. Lett.* **93**, 086802 (2004); O. Mitrofanov, D. V. Lang, C. Kloc, J. M. Wikberg, T. Siegrist, W. Y. So, M. A. Sergent, and A. P. Ramirez, *ibid.* **97**, 166601 (2006); C. Krellner, S. Haas, C. Goldmann, K. P. Pernstich, D. J. Gundlach, and B. Batlogg, *Phys. Rev. B* **75**, 245115 (2007).
- ⁹A. F. Stassen, R. W. I. de Boer, N. N. Iosad, and A. F. Morpurgo, *Appl. Phys. Lett.* **85**, 3899 (2004).
- ¹⁰I. N. Hulea, S. Fratini, H. Xie, C. L. Mulder, N. N. Iosad, G. Rastelli, S. Ciuchi, and A. F. Morpurgo, *Nature Mater.* **5**, 982

(2006).

- ¹¹J. Takeya *et al.*, *Phys. Rev. Lett.* **98**, 196804 (2007).
- ¹²M. Fischer, M. Dressel, B. Gompf, A. K. Tripathi, and J. Pflaum, *Appl. Phys. Lett.* **89**, 182103 (2006); Z. Q. Li, V. Podzorov, N. Sai, M. C. Martin, M. E. Gershenson, M. Di Ventra, and D. N. Basov, *Phys. Rev. Lett.* **99**, 016403 (2007).
- ¹³K. P. Pernstich, B. Rossner, and B. Batlogg, *Nature Mater.* **7**, 321 (2008).
- ¹⁴C. Reese and Z. Bao, *Adv. Mater.* **19**, 4535 (2007).
- ¹⁵V. Podzorov, V. M. Pudalov, and M. E. Gershenson, *Appl. Phys. Lett.* **82**, 1739 (2003); V. Podzorov, S. E. Sysoev, E. Loginova, V. M. Pudalov, and M. E. Gershenson, *ibid.* **83**, 3504 (2003).
- ¹⁶J. Takeya, C. Goldmann, S. Haas, K. P. Pernstich, B. Ketterer, and B. Batlogg, *J. Appl. Phys.* **94**, 5800 (2003); V. Y. Butko, X. Chi, D. V. Lang, and A. P. Ramirez, *Appl. Phys. Lett.* **83**, 4773 (2003).
- ¹⁷R. W. I. de Boer, T. M. Klapwijk, and A. F. Morpurgo, *Appl. Phys. Lett.* **83**, 4345 (2003); V. Y. Butko, X. Chi, and A. P. Ramirez, *Solid State Commun.* **128**, 431 (2003); H. E. Katz, C. Kloc, V. Sundar, J. Zaumseil, A. L. Briseno, and Z. Bao, *J. Mater. Res.* **19**, 1995 (2004).
- ¹⁸S. Fratini, H. Xie, I. N. Hulea, S. Ciuchi, and A. F. Morpurgo, *New J. Phys.* **10**, 033031 (2008).
- ¹⁹A. S. Molinari, I. Gutiérrez Lezama, P. Parisse, T. Takenobu, Y. Iwasa, and A. F. Morpurgo, *Appl. Phys. Lett.* **92**, 133303 (2008).
- ²⁰T. Kaji, T. Takenobu, A. F. Morpurgo, and Y. Iwasa, *Adv. Mater.* **21**, 3689 (2009).

- ²¹I. Gutiérrez Lezama and A. F. Morpurgo, *Phys. Rev. Lett.* **103**, 066803 (2009).
- ²²W. Warta and N. Karl, *Phys. Rev. B* **32**, 1172 (1985).
- ²³G. Horowitz, M. E. Hajlaoui, and R. Hajlaoui, *J. Appl. Phys.* **87**, 4456 (2000).
- ²⁴M. F. Calhoun, C. Hsieh, and V. Podzorov, *Phys. Rev. Lett.* **98**, 096402 (2007).
- ²⁵M. S. Nam, A. Ardavan, R. J. Cava, and P. M. Chaikin, *Appl. Phys. Lett.* **83**, 4782 (2003).
- ²⁶J.Y. Kim, M. Yun, D.-W. Jeong, J.-J. Kim, and I. J. Lee, *J. Korean Phys. Soc.* **55**, 212 (2009).
- ²⁷E. Menard, V. Podzorov, S.-H. Hur, A. Gaur, M. E. Gershenson, and J. A. Rogers, *Adv. Mater.* **16**, 2097 (2004).
- ²⁸To see examples in which this strategy has been applied to the analysis of transistor data in amorphous organic materials, see, for instance, A. Salleo, T. W. Chen, A. R. Volkel, Y. Wu, P. Liu, B. S. Ong, and R. A. Street, *Phys. Rev. B* **70**, 115311 (2004); J. A. Merlo *et al.*, *J. Am. Chem. Soc.* **127**, 3997 (2005); For other related work, see, for instance, D. Oberhoff, *et al.*, *IEEE Trans. Electron Devices* **54**, 17 (2007).
- ²⁹A. Troisi and G. Orlandi, *Phys. Rev. Lett.* **96**, 086601 (2006).
- ³⁰K. Hannewald and P. A. Bobbert, *Appl. Phys. Lett.* **85**, 1535 (2004).
- ³¹Presently, our analysis cannot discriminate between small differences in the value of the exponent, which depend on details of the theoretical models.
- ³²E. A. Silinsh and V. Capek, *Organic Molecular Crystals* (AIP, New York, 1994).
- ³³For a general overview, see Chapter 12 of Y. Roichman *et al.*, *Physics of Organic Semiconductors* (Wiley, New York, 2005), and references therein.
- ³⁴M. C. J. M. Vissenberg and M. Matters, *Phys. Rev. B* **57**, 12964 (1998).
- ³⁵As an example of the possibility to check the consistency of the results, we note that the model discussed in this paper—and similar models used previously—relies essentially on the concept of “mobility edge” (i.e., on the existence of an energy value separating states that, when filled, contribute to conduction, from states that are localized and do not contribute to the conduction). In amorphous materials, this is an assumption that is not checked experimentally, because a metalliclike mobility is not observed in the measurements.
- ³⁶We have obtained similar and consistent results also with an exponential distribution. With such a distribution, however, the threshold voltage below 100–150 K is suppressed much more rapidly than with the constant or Gaussian distributions.
- ³⁷If we assume that the deep traps that affect transport at the surface of the crystals are located within a distance of only a few molecules from the crystal surface (say 5–10 nm), we can use the parameter N_D extracted from the fits, to estimate a volume density of states for the deep traps. We obtain values on the order of $10^{17} \text{ cm}^{-3} \text{ eV}^{-1}$, which compare well with densities previously found in the *bulk* of rubrene and pentacene crystals (Ref. 8) (see also Fig. 5 of D. Braga and G. Horowitz, *Adv. Mater.* **21**, 1473 (2009)). Since the density of defects at the crystal surface is expected to be larger than in the bulk (for the case of rubrene, see Ref. 11), this indicates the high quality of the TMTSF crystals.
- ³⁸To avoid misunderstandings, we emphasize that our model does not attempt to capture the contribution to the conductivity due to the carriers occupying shallow traps. This contribution is negligible as long as enough carriers are present in the band, which is the case for temperatures higher than approximately 100 K in the best devices. In this range, we can then safely ignore the current carried by carriers that occupy shallow traps. However, in the lowest temperature range ($T < 100 \text{ K}$ in the best devices, i.e., the range excluded from our analysis), the amount of carriers occupying states in the band becomes negligible. Nevertheless, the conductivity that is observed experimentally remains rather high (with mobility values still as high as $\approx 2 \text{ cm}^2/\text{V s}$ at 50 K in the best devices). This indicates that carriers in shallow traps do still carry current. Qualitatively, our picture of shallow traps as extended regions where the energy of the electrons is low because of the electrostatic potential fluctuations is consistent with this conclusion. In fact, in this scenario, carriers in shallow traps move in the extended regions and contribute to the local conductivity.